J Infrared Milli Terahz Waves (2012) 33:17–24
DOI 10.1007/s10762-011-9834-1

Construction and Measurement of a 31.3–45 GHz Optimized Spline-profile Horn with Corrugations

Pablo Zorzi · Christophe Granet · Franco Colleoni · Nicolas Reyes · Jose Pizarro · Fausto-Patricio Mena · Leonardo Bronfman

Received: 28 July 2011 / Accepted: 13 September 2011 /
Published online: 7 October 2011

Abstract A corrugated spline-profile horn has been designed to meet the stringent specifications and constraints of a receiver for Band 1 (31.3–45 GHz) of the Atacama Large Millimeter Array (ALMA). Given the physical restrictions of the receiver, the horn will be located behind a focusing lens placed 191 mm over its aperture. After this first focusing stage, the horn must have a reflection coefficient less than −20 dB and the cross-polarization not exceeding the −30 dB level in the entire frequency range. The side-lobes should be less than −25 dB at all frequencies and its half power beamwidth must be approximately 24° at 31.3 GHz and 16° at 45 GHz. The horn has been constructed using the split-block technique and characterized in a near-field scanner setup. The results show an excellent performance complying with all the requirements.

Keywords Spline-profile · Corrugated horn · Radiation pattern · Cross-polarization · Phase center · Quasi optics · Radio receiver

P. Zorzi (✉) · F. Colleoni · N. Reyes · F. P. Mena
Department of Electrical Engineering, Universidad de Chile,
Av. Tupper 2007, Santiago, Chile
e-mail: pzorzi@ing.uchile.cl

C. Granet
BAE Systems Australia Pty Ltd, 40-52 Talavera Road, North Ryde, 2113 NSW, Australia

J. Pizarro · L. Bronfman
Astronomy Department, Universidad de Chile, Camino el Observatorio,
1515, Las Condes, Chile

1 Introduction

The Atacama Large Millimeter Array (ALMA) is the largest millimeter and sub-millimeter astronomical array ever built. It is under construction in the altiplano region of northern Chile. This is an extremely dry plateau at an altitude of 5,000 m, making it one of the best sites on earth for radio astronomy. ALMA combines an array of 66 antennas (54 × 12 m and 12 × 7 m diameter antennas) designed to perform interferometry and spectroscopic measurements of the early Universe with an angular resolution accuracy of 1" [1]. It will also reveal new information about the birth of stars and planets and the formation of galaxies. In general, ALMA will provide high sensitive and precision imaging between 30 and 950 GHz in 10 bands of the Southern Hemisphere sky (http://almascience.eso.org/alma-science). This telescope will be already functional in 2011 although with only 16 antennas and 4 bands implemented.

The aim of this paper is to present the details of the design, construction and testing of a 31.3 45 GHz spline-profile corrugated horn that will be used in an ALMA Band-1 receiver. The horn is used to feed a high-density polyethylene (HDPE) bi-hyperbolic lens 194 mm in diameter and located at 191 mm from the aperture of the horn. Furthermore, the outgoing radiation from the lens will subsequently illuminate a 750 mm diameter subreflector, located 5.79 m from it, with a uniform Gaussian beam efficiency of −12.3 dB at all frequencies.

2 Design

In order to achieve the stringent specifications imposed over the horn, in particular its large coverage bandwidth, two different profiles were studied using mode-matching techniques and the optimization procedure defined step by step in [2] and [3]. The first was based on a smooth-walled profile while the

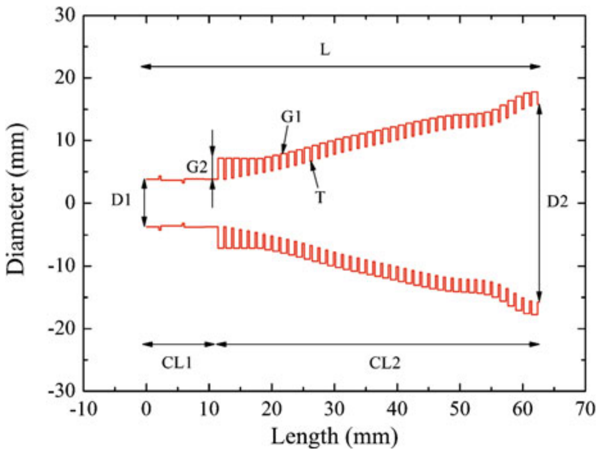

Fig. 1 Profile of the spline-profile corrugated horn. The dimensions are given in Table 1.

Table 1 Dimensions of the different sections of the corrugated horn.

Index	Section	Dimension (mm)
L	Horn total length	62.37
CL1	Circular waveguide length	11.42
CL2	Corrugated section length	51.25
D1	Input diameter	7.62
D2	Output diameter	31.50
T	Teeth width	0.94
G1	Grove width	0.31
G2	Grove depth	2.01–3.35

second model used was a corrugated spline-profile horn. As it was shown in [4], the spline-profile corrugated horn design was the best choice to construct since it met all the specifications in a much better way than the simple smooth-walled horn. As an additional advantage, the corrugated spline-profile horn resulted in a total length which is almost half of that of the conventional conical corrugated horn [5], making it easier to be implemented in the Band-1 receiver. This is particularly important in ALMA as the available space for implementing the receiver is limited [6]. After the design, all the results were corroborated using HFSS (http://www.ansoft.com/products/hf/hfss). The corrugation profile of the selected horn is shown in Fig. 1 and Table 1 summarizes its physical dimensions.

3 Construction

The spline-profile corrugated horn was constructed using the split-block technique. Both split sections were milled using a five-axis high-precision CNC milling machine (http://www.kern-microtechnic.com). The horn was milled in aluminum due to its good machinability and suitability for cryogenic applications. The corrugation profile at the split plane was checked with an optical microscope. No construction errors and misalignment of the corrugations were found. This sets the construction and alignment precision in less than 10 mm.

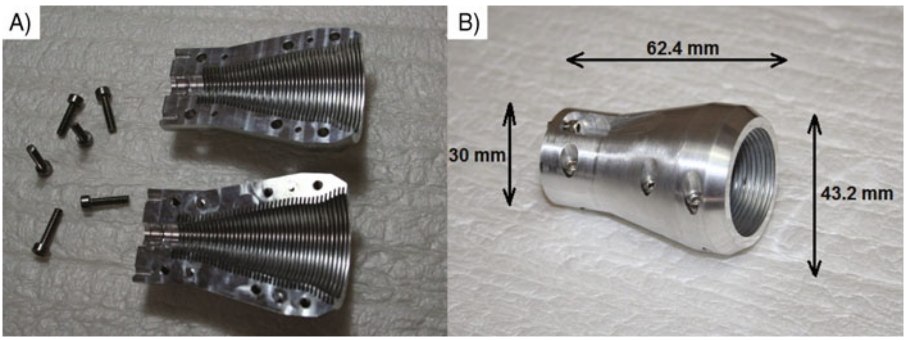

Fig. 2 Fabricated horn. **a** The two split-block halves. **b** Assembled horn and final dimensions.

Instead of using standard alignment pins, four pins were machined directly in one of the block surfaces minimizing in this way the alignment errors once the horn was assembled. The horn is presented in Fig. 2.

4 Measurements, results, and discussions

For the characterization of the horn, a vertical planar near-field beam-pattern measurement setup was designed and built [7, 8]. The near to far-field data transformation algorithm, which uses a Fast Fourier Transform (FFT) on the near-field measured data, and the probe amplitude pattern corrections were adapted from [9]. The resulting measured far-field data were consistent within a dynamical range of greater than 50 dB. For determining the phase center a phase model with amplitude weighting correction was used [10]. In this section we present the measured reflections at all frequencies, and the co-polar and cross-polar radiation pattern, phase and phase center location at 31.3, 38 and 45 GHz. All the measured data presented here includes the corresponding HFSS simulations for comparison purposes.

4.1 Reflection coefficient

Figure 3 presents the measured reflection losses at the input port of the horn. The measurements correspond to the real circular waveguide input. The contribution of the rectangular-to-circular waveguide transition was subtracted using a previous calibration step. The measurements show that the reflection losses are less than −20 dB for the complete band of interest in excellent agreement with the simulations.

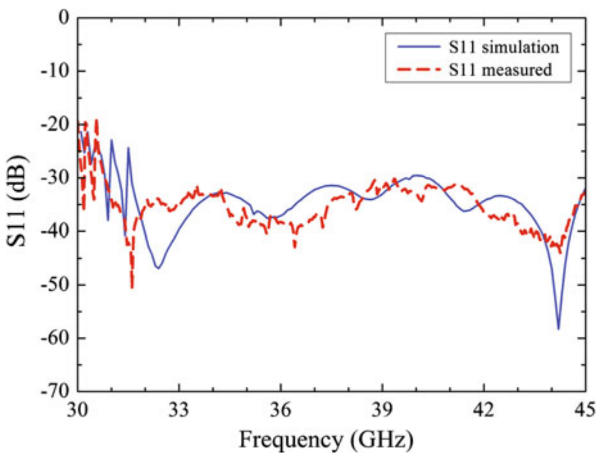

Fig. 3 Measurements of the horn input reflections (*red line*) compared to the HFSS simulated expected S11 values (*blue line*).

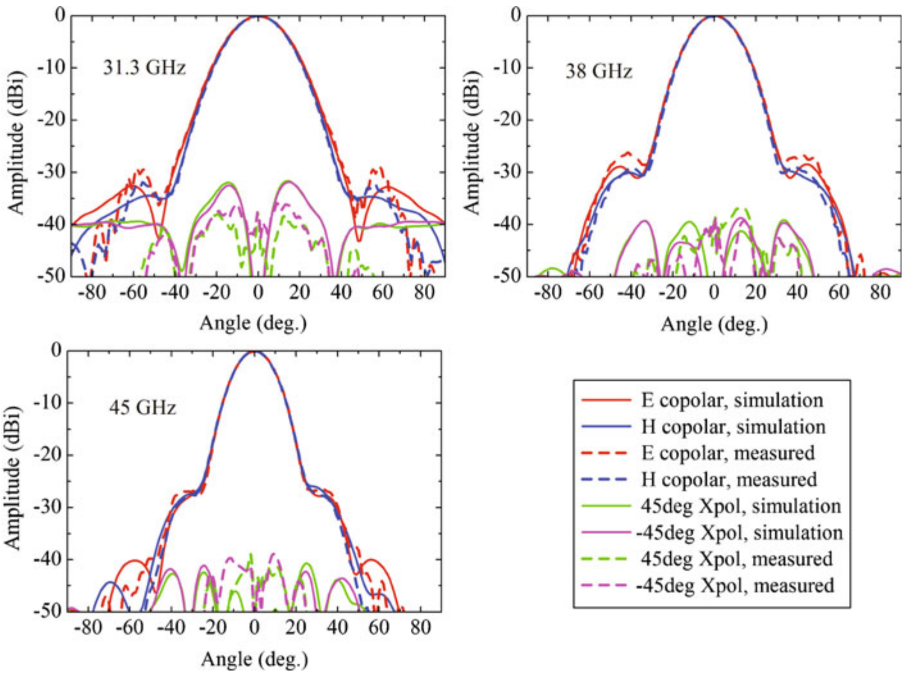

Fig. 4 Measured and simulated co-polar (E and H planes) and cross-polar (45 and −45 planes) radiation pattern comparison for 31.3, 38 and 45 GHz. *Dotted lines* correspond to the measurements results while the *straight lines* corresponds to the simulation results.

4.2 Co- and cross-polar patterns

The co-polar and cross-polar radiation patterns are shown in Fig. 4. The copolar measurements are identical to the simulated ones down to −25 dB at all frequencies. At lower amplitude values, especially around the first sidelobe levels, the measurements are always somewhat large with respect to the simulations. The difference in cross-polar amplitude between the simulations and measurements, especially at 38 and 45 GHz, are of about +5 dB. However, all the cross-polar and first sidelobe level measurements fulfill the horn-performance specifications.

4.3 Directivity and level of the first side-lobe

From the simulated and measured radiation patterns we have obtained the directivities and the levels of the first side-lobes. The results are summarized in Figs. 5 and 6. In both cases, the measured and simulated values show similar frequency dependence. In the case of the measured directivities, they are slightly overestimated in around 0.3 dB for each case. This is probably due to the uncertainty when predicting the total isotropic radiated power of our horn from the planar near-field measurement once the far-field transformation is

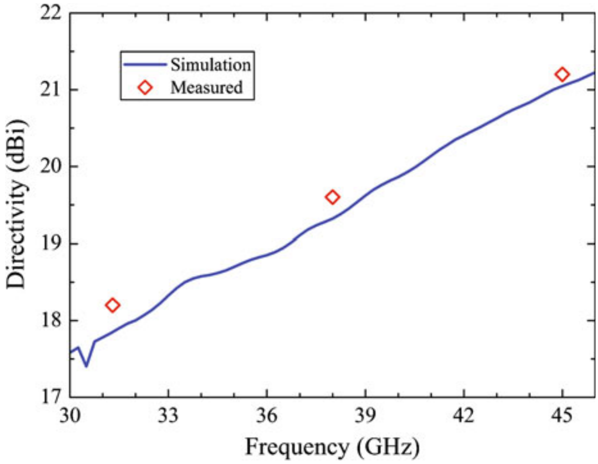

Fig. 5 Measured and predicted directivity of the constructed horn.

done using the FFT methods. Regarding the first side-lobe level, it is typically below −26 dB across the whole band, which implies that the specifications set for the horn are satisfied.

4.4 Phase plots and phase center location

The measured phase of the E and H fields and their corresponding simulated HFSS values at 31.3, 38 and 45 GHz are shown in Fig. 7. The measured results agree very well with the simulations since the phase diagrams are quite flat in the region where the amplitude radiation reaches its maximum. In Fig. 8 the phase center location (PCL) retrieved from the measured and simulated cases are presented. The measured PCLs coincide with the simulated cases

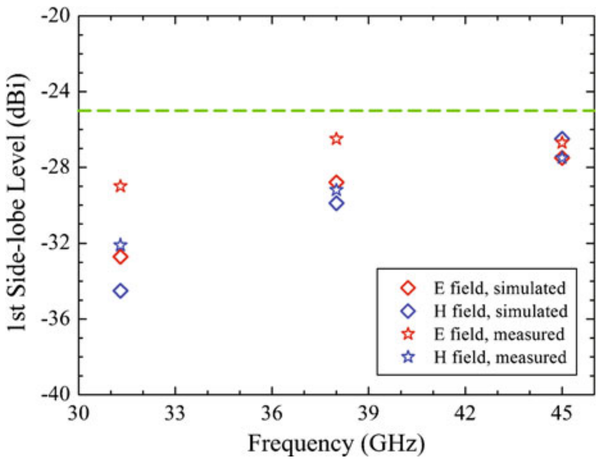

Fig. 6 Measured and simulated first side-lobe levels. The *green dotted line* denotes the maximal first side-lobe level specification of the horn.

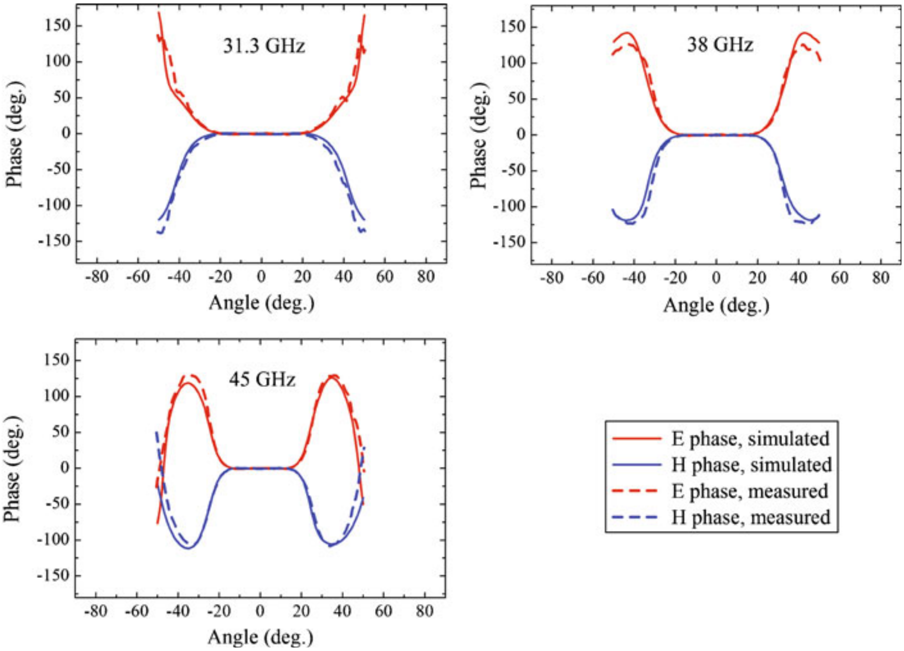

Fig. 7 Measured and simulated phase plots results for the E (*red lines*) and H planes (*blue lines*) at 31.3, 38 and 45 GHz.

within about 0.5 mm. The exception is the PCL of the H-field at 45 GHz, where the difference with its corresponding simulated value is of about 1.5 mm. This discrepancy may be attributed to small construction imperfections in the corrugation profile which is more sensitive at higher frequencies.

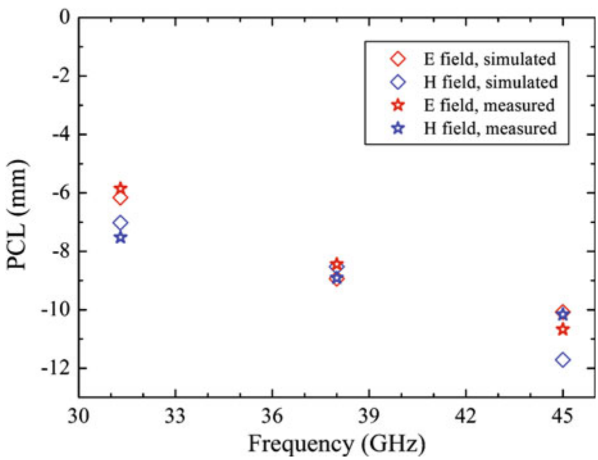

Fig. 8 Measured and simulated phase center locations for the E (*red*) and H fields (*blue*).

5 Conclusions

We have successfully constructed a spline-profile optimized corrugated horn using split-block techniques. The measurements of its return losses, directivity, first side-lobe levels, and its co- and cross-polar radiation pattern measurements agree very well with the HFSS simulation results and fulfill all the required specifications imposed by ALMA for its Band 1. The measured phase and phase-center location of the horn show similar deviations from the HFSS simulation. Furthermore, it was demonstrated that the construction discontinuities, due to the horn being split in two parts, were negligible and causes no detectable anomalies in the cross polar measured pattern. This construction technique is, therefore, suitable and could replace electroplating techniques. Another advantage of the horn design is that it has a similar or even better performance than a standard corrugated horn design but with almost half its size. This is an important mechanical achievement since the space in an ALMA receiver is limited.

Acknowledgements This work was supported by the Chilean Center of Excellence in Astrophysics and Associated Technologies (PBF 06), and by the ALMA-CONICYT Fund for the Development of Chilean Astronomy (Projects 31080003 and 31080004).

References

1. H. Rudolf, M. Carter, and A. Baryshev, “The ALMA Front End Optics-System Aspects and European Measurement Results,” IEEE Transactions on Antennas and Propagation, Vol. 55, No. 11, November 2007.
2. C. Granet, G.L. James, R. Bolton, G. Moorey, “A smooth-walled spline-profile horn as an alternative to the corrugated horn for wide band millimeter-wave applications,” IEEE Transactions on Antennas and Propagation, Vol. 52, No. 3, March 2004, pp. 848–854.
3. C. Granet, T.S. Bird, “Optimization of corrugated horn radiation patterns via a spline-profile,” ANTEM 2002, 9th International Symposium on Antenna Technology and Applied Electromagnetics, Montreal, Canada, 2002, pp 307–310.
4. C. Granet, P. Mena, P. Zorzi, I.M. Davis, J.S. Kot, G. Pope, “Corrugated and Smooth-Walled Spline-Profile 31.3–45 GHz Horns for ALMA.” Proceedings of the 4th European Conference on Antennas and Propagation, Barcelona, Spain, 12–16 April 2010.
5. C. Granet and G. L. James, “Design of corrugated horns: A primer,” IEEE Antennas & Propagation Magazine, Vol. 47, No 2, April 2005, pp. 76–84. (Correction in IEEE Antennas & Propagation Magazine, Vol. 47, No 4, August 2005, p. 98).
6. ALMA Front-end Optics Design Report. Document: FEND-40.02.00.00-035-B-REP.
7. S. Gregson, J. McCormick and C. Parini, “Principles of Planar Near-Field Antenna Measurements.” Institution of Engineering and Technology Press, 2007.
8. T. Brockett and Y. Rahmat-Samii, “A Novel Portable Bipolar Near-field Measurement System for Millimeter-wave Antennas: Construction, Development, and Verification,” IEEE Antennas and propagation Magazine, Vol. 50, No. 5. October 2008.
9. D. Janse van Rensbur, “Millimeter Wave Near-Field Antenna Testing.” Nearfield Systems Inc. Microwave Product Digest Article, Aug 2010.
10. P.N. Betjes, “An algorithm for automated phase center determination and its implementation,” AMTA Conference, 2007.